ARC Centre of Excellence in Population Ageing Research

Working Paper 2019/15

A Value-Based Longevity Index for Hedging Retirement Income Portfolios

Kevin Krahe, Michael Sherris, Andrés M. Villegas and Jonathan Ziveyi

---

A Value-Based Longevity Index for Hedging Retirement Income Portfolios

Kevin Krahe*, Michael Sherris†, Andrés M. Villegas‡and Jonathan Ziveyi§

October 3, 2019

Abstract

We develop and assess a value-based longevity index that closely tracks the value of longevity-linked liabilities with the potential to significantly lower the costs and improve the efficiency of index-based longevity hedging techniques relative to standard mortality rate indices, currently referenced in financial markets. As the US is one of the largest countries in terms of market potential for such an index, we use US economic and population data to demonstrate that hedging with our proposed index generates a material reduction in basis risk relative to indices based purely on mortality rates. This is aided by the use of a multi-population continuous-time affine mortality model and a dynamic Nelson-Siegel model for interest rates. We allow both interest rate and inflation risks to impact the value of longevity-linked liabilities in our longevity risk hedging. We also bridge the gap between continuous-time and discrete-time multi-population mortality models and show that the continuous-time models are as effective in hedging liabilities as the often used discrete-time models, while being more familiar to financial market participants.

Keywords: Value-based longevity index, longevity risk, interest rate risk, inflation risk, longevity basis risk, longevity hedging

*Email: kevin.krahe@gmail.com

†Email: m.sherris@unsw.edu.au; Phone: +61 2 9385 2333 UNSW Business School, Risk and Actuarial Studies, Centre of Excellence in Population Ageing Research (CEPAR), UNSW Sydney, NSW 2052, Australia.

‡Email: a.villegas@unsw.edu.au; Phone: +61 2 9385 2647; UNSW Business School, Risk and Actuarial Studies, CEPAR, UNSW Sydney, NSW 2052, Australia.

§Email: j.ziveyi@unsw.edu.au; Phone: +61 2 9385 8006; UNSW Business School, Risk and Actuarial Studies, CEPAR, UNSW Sydney, NSW 2052, Australia.

1 Introduction

Retirement income providers such as defined benefit pension funds and annuity providers are heavily exposed to longevity risk - the potential unexpected increase in life expectancy of pensioners and life annuity holders. Some estimates suggest that each additional year of life expectancy increases annual pension liability values by 3 to 4 percent (International Monetary Fund, 2012; Chang and Sherris, 2018). The world's aggregate longevity risk exposure is growing rapidly. The 2018 Global Pension Assets Study by Willis Towers Watson (2018) reports that the value of defined benefit pension assets has grown by 4.5% per year over the last 20 years, and was valued at US$21.3 trillion as of February 2018. The Joint Forum (2013) highlights that each year of life expectancy underestimation could potentially cost risk holders up to US$1 trillion in additional unexpected benefit payments.

The traditional approach to managing longevity risk is through the transfer of liabilities to life insurance or reinsurance companies (Coughlan et al., 2011). This can be achieved through either a pension buy-in or a pension buy-out, as described in Blake et al. (2018). However, with consistent growth in retirement income liability volumes over recent years, the world's aggregate longevity risk exposure is approaching the global insurance industry's finite capacity for longevity risk absorption (Barrieu et al., 2012; Joint Forum, 2013). Furthermore, regulations such as Solvency II have enhanced the demand for longevity reinsurance as a means of reducing solvency capital requirements (Xu et al., 2019).

In recent years, the development of a longevity risk transfer market has emerged as a potential solution, with the development of various mortality and longevity-linked indices, instruments and derivative securities. The risk transfer and capital market database Artemis (2019)[1] has documented at least 91 longevity-linked transactions completed as of September 2019, collectively valued at an aggregate amount of over £180 billion with transaction sizes growing over time since the first ever transaction took place in January 2008 between J.P. Morgan and UK insurer Lucida. Most transactions to date have been customised or "bespoke" indemnity swaps, that is, customised over-the-counter hedges that transfer a retirement income provider's specific longevity risk exposure to a counterparty.

In bespoke transaction, there is no longevity basis risk associated with the hedge for the retirement income provider as the counterparty effectively assumes all obligations arising from the exposure. From an economic perspective, an indemnity hedge is identical to the traditional approach of transferring the annuity book to a life insurer or reinsurer, however in the format of a capital market instrument (Coughlan, 2009). The major drawback is the need for investors to analyse fund-specific details on the portfolio being hedged. This makes it complex and costly for capital markets to evaluate potential transactions, thereby discouraging investors and inhibiting the development of market liquidity (Coughlan, 2009).

By contrast, a standardised index-based hedge is based on the mortality experience over time of some underlying "reference" population as represented by a published longevity index. For example, in 2007 J.P. Morgan launched the Lifemetrics Index[2] which provides male and female period life expectancies, crude central mortality rates and graduated initial mortality rates for the US, England and Wales, the Netherlands and Germany

[1] www.artemis.bm/library/longevity_swaps_risk_transfers.html

[2] https://llma.org/index/index-description/

(Coughlan et al., 2007). From 2010, the management of the Lifemetrics Index is under the Life and Longevity Markets Association (Life and Longevity Markets Association, 2018). Another well known longevity index is the Xpect-Club Vita Index[3] launched by Deutsche Börse in March 2008 (Deutsche Börse, 2018).

It is critical that any longevity index intended for index-hedging purposes is transparent, objective and can serve as an unbiased point of reference for all participants in the longevity risk transfer market (Loeys et al., 2007; Sweeting, 2010). In contrast to indemnity hedges, index hedges do not require the analysis of portfolio-specific details; cashflows only depend on population-level mortality experience as represented by the published longevity index which makes it much simpler for investors to understand and manage the associated risks. Therefore, these instruments have a much greater potential to develop sufficient market liquidity over time and become viable longevity risk transfer vehicles (Villegas et al., 2017). However, longevity index-based instruments cannot hedge the specific mortality experience of a given retirement income portfolio or "book". That is, they are subject to longevity basis risk – an issue which remains a major barrier to index-based hedging solutions (Coughlan et al., 2007). Our research is primarily motivated by this critical need to minimise the basis risk associated with such hedging techniques.

The Longevity Basis Risk Working Group (LBRWG) notes that in addition to the prevalence of longevity basis risk, the lack of a robust framework for quantifying longevity basis risk has further impeded the appetite for standardised index-based longevity hedging solutions. In order to tackle this issue, the LBRWG commissioned a major research project to develop a methodology for assessing basis risk in longevity transaction as documented in the Phase 1 (Haberman et al., 2014) and Phase 2 (Li et al., 2017) technical reports of the research. These technical reports, which are complemented by scholarly research (see Villegas et al. (2017) and Li et al. (2019)) propose techniques to quantify each of the three constituent of longevity basis risk described in Mosher and Sagoo (2011), namely:

(i) *Structuring basis risk* resulting from differences in the timing or maturity of cashflows between the hedging instrument to that of the annuity liability which is incorporated using numerical optimisation procedures,

(ii) *sampling basis risk* arising from the random variation around expected mortality outcomes in finite book sizes is quantified by implementing random sampling techniques, and

(iii) *demographic basis risk* resulting from socio-economic or demographic differences between the composition of the reference and book populations is modelling through multi-population mortality modelling frameworks.

Our research seeks to complement the work of the LBRWG by proposing a value-based longevity index and a novel continuous-time approach for quantifying the resulting basis risk.

To quantify demographic basis risks it is necessary to capture the mortality dependence structure among the different populations relevant to the the longevity transaction. This is typically achieved by fitting multi-population mortality models to the mortality data of the different populations, modelling their relationship over time and projecting their joint

[3] `http://www.xpect-index.com`

mortality outcomes into the future. Most multi-population mortality models described in the literature are constructed in discrete-time, with a comprehensive overview of the "universe" of such models detailed in Villegas et al. (2017). However, the literature on applications of continuous-time multi-population mortality modelling is much less developed. To the best of our knowledge, the models proposed in Jevtić and Regis (2019) and Xu et al. (2019) are some of the few continuous-time multi-population mortality models proposed to date. This is in spite of the fact that, relative to discrete-time models, the continuous-time class of mortality models offer vastly superior versatility in applications involving financial modelling (Jevtić et al., 2013). Furthermore, no research has yet directly compared hedging outcomes under the two types of multi-population mortality modelling frameworks, providing scope for our research to offer a novel contribution to the existing literature.

Retirement income providers are not only exposed to longevity risk, but also interest rate and inflation risks (Towers Watson, 2013). However, to date, index-based longevity hedging transactions have referenced longevity indices linked to national life tables such as the Lifemetrics Index which fails to incorporate these other critical sources of risk (Cairns, 2017). This has been a key motivation for Sherris (2009) who highlights the need for value-based longevity indices which aim to track the expected present value of a unit of longevity-indexed income. Unlike life tables-based survival rate indices, value-based longevity indices have the capacity to integrate all of the major risk factors associated with the provision of retirement income products (Wills and Sherris, 2010). Therefore, such indices should intuitively be associated with lower levels of structuring basis risk when used to underlie standardised longevity hedging transactions, particularly if they are designed in such a way as to reflect the major sources of risk associated with retirement income portfolios which is a central hypothesis of this paper.

Xu et al. (2019) construct value-based longevity indices based on uncertain interest rates and mortality dynamics of Australia, the UK, the Netherlands and France. Despite not explicitly modelling sampling nor structuring basis risk, their analysis demonstrates that interest rate risk is a material element in the hedging framework, implying that value-based longevity indices have the capacity to improve hedging outcomes through their potential to incorporate interest rate uncertainty in addition to longevity risk. Similarly, Chang and Sherris (2018) find that the basis risk associated with an index swap referencing a value-based longevity index is significantly lower than that of an S-forward based on population survival rates in stochastic interest rate settings. While the analysis in Chang and Sherris (2018) does not incorporate demographic basis risk nor inflation-indexation of retirement benefits, it demonstrates the potential for value-based longevity indices to significantly improve standardised longevity hedging outcomes. This paper seeks to extend on these analyses by explicitly addressing all three constituent components of longevity basis risk in the evaluation of index-based hedging of retirement income portfolios.

In 2013, the global asset manager BlackRock launched the Cost of Retirement Index (CoRI)[4] for twenty US cohorts; a set of value-based longevity indices which track the cost of an inflation-indexed retirement income stream while incorporating the market price of longevity risk as reflected in the prevailing prices of retirement income products. However, as Sweeting (2010) notes, longevity indices that are used for index hedging applications must be calculated in an objective and transparent manner. Since retirement income providers are able to directly influence the CoRI through their pricing policies, the index would not be perceived as an independent, objective representation of longevity outcomes

[4] `https://www.blackrock.com/cori/fact-sheets`

if used to underlie standardised capital market instruments.

The contribution of this paper is threefold. Firstly, while various value-based longevity indices have been proposed and constructed in the literature, to date none have incorporated all three of the major risk factors associated with retirement income portfolios; that is, longevity risk, interest rate risk and inflation risk (Towers Watson, 2013). We expect to fill this literature gap by providing a template for the development of an index that closely tracks the value of longevity-linked liabilities, fulfilling a key need of practitioners in the longevity risk transfer market. Furthermore, by constructing such an index, the attribution of risk among these three elements can be estimated.

Various authors have assessed the basis risk associated with value-based longevity indices, none have engaged the holistic, decomposed quantification framework developed by the LBRWG. For example, Xu et al. (2019) account for demographic basis risk in their analysis, while Chang and Sherris (2018) incorporate sampling basis risk. By assessing all three constituent components of longevity basis risk, our second contribution fills this important literature gap and contribute towards the robust evaluation of index-based longevity hedging in industry. Indeed, we present compelling evidence of reduced basis risk for the value-based longevity index relative to standard survival rate indices.

Finally, while both discrete-time and continuous-time multi-population mortality modelling techniques have been developed, no work has compared the hedging outcomes associated with the two different classes of models. Our third contribution fills this gap where we note that despite their significant methodological differences, the two modelling frameworks ultimately suggest relatively comparable hedging outcomes – a contribution which additionally facilitates the assessment of model risk on hedge outcomes which is another key consideration for practitioners.

The remainder of this paper is organised as follows. Section 2 introduces the proposed value-based longevity index. Subsection 2.1 details both the continuous-time and discrete-time mortality models utilised in this paper, while the interest rate modelling framework is described in Subsection 2.2. The liability profile of the retirement income portfolio is presented in Section 3. Section 4 presents numerical illustrations for the value-based longevity index. Section 5 introduces an index swap instrument and designs a hedging strategy to calibrate the optimal notional swap weighting. Section 6 presents several basis risk measures to compare the hedge effectiveness of the value-based longevity index relative to a variety of indices with various specifications to highlight the additional risk reduction generated by the proposed index. Section 7 presents a range of sensitivity analyses to determine the significance of various modelling assumptions and experimental design settings. Finally, Section 8 concludes the paper.

2 Value-Based Longevity Index

This paper considers the construction of a value-based longevity index, $I_{x,t}$, which quantifies the expected present value of a unit of longevity and inflation indexed income paid annually in arrears to a cohort aged, x, at initial time, t. As it accounts for all three main risk factors associated with retirement income portfolios, the index is able to more efficiently track the value of longevity-linked liabilities; the ability to simultaneously hedge longevity risk, interest rate risk and inflation risk with a single product fulfils a key need

of practitioners in the longevity risk transfer market. The value of the index is represented as

$$I_{x,t} = \sum_{i=1}^{\omega-x} S^R(x,t,t+i) \times P_R(t,t+i),$$

where ω is the maximum attainable age. The quantity $S^R(x,t,t+i)$ denotes the i year survival probability of the population underlying the index, and is forecast using the mortality modelling frameworks described in Subsection 2.1. The quantity $P_R(t,t+i)$ denotes the time t price of an inflation-indexed zero coupon bond making a single unit payment at time $t+i$, and is forecast using the interest rate modelling techniques presented in Subsection 2.2. The functional forms of the forecast survival probabilities and bond prices, $S^R(x,t,t+i)$ and $P_R(t,t+i)$, are presented in Subsections 2.1 and 2.2 respectively.

The population whose mortality underlies the value-based longevity index is termed the "reference" population and is distinguished from the "book" population which refers to the retirement income portfolio to be hedged against the index. In order to capture their dependence in longevity experience, the mortality dynamics of the two populations are jointly modelled in Subsection 2.1.

In contrast to the BlackRock's CoRI[5], which is influenced by prevailing pricing of retirement income products by providers, the value-based longevity index does not incorporate any longevity risk premium, reflecting only the forecast survival rates, interest rates and inflation. This ensures that market participants view the index as an independent, objective representation of longevity outcomes, which is a critical requirement for a viable index-based longevity risk transfer market (Sweeting, 2010). Financial markets are left to determine an appropriate price for longevity risk through the setting of forward prices for traded index-linked instruments. Furthermore, in accordance with Chang and Sherris (2018), the index does not account for any expense loading or profit margin.

2.1 Mortality Modelling Framework

Despite the well-developed literature on discrete-time multi-population mortality modelling, continuous-time models have not been explored much regardless of their enormous flexibility in applications when integrated with other financial modelling elements (Jevtić et al., 2013). For the mortality modelling framework, we adopt the multi-factor joint affine term structure model (ATSM) as developed in Xu et al. (2019). This model is inspired by multi-country affine term structure interest rate models which have proved to be flexible, tractable and exhibit exceptional empirical fit (Christensen et al., 2011). Furthermore, the affine term structure framework provides explicit closed-form solutions for survival probabilities as a function of the underlying factors, which significantly simplifies our computational process.

In explaining the mortality dynamics of the two populations, three latent time-varying factors are incorporated into the modelling framework; a local factor $R_{x,t}$ which only impacts the mortality of the reference population R, another local factor $B_{x,t}$ which only impacts the mortality of the book population B and a common factor $C_{x,t}$ which affects the mortality dynamics of both the reference and book populations. These three factors are depicted in red, blue and red-blue combined circles in Figure 1 respectively, with arrows

[5] `https://www.blackrock.com/cori/fact-sheets`

denoting their respective impacts on each of the two populations modelled. The reference and book populations are depicted as red ("R") and blue ("B") rectangles respectively.

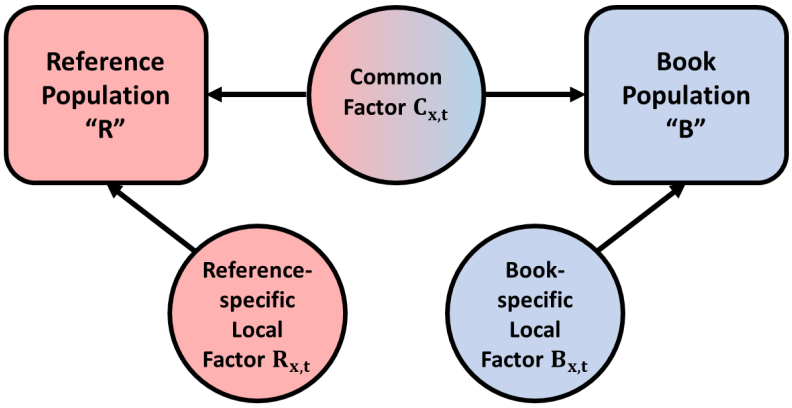

Figure 1: Structure of the joint affine term structure model for mortality.

From this diagram, it is apparent that the common factor captures all the dependence in mortality experience across the two populations arising from their mutual exposure to certain common influences (for example, a strong winter). Conversely, the two local factors facilitate discrepancies in mortality dynamics over time between the two populations owing to differences in their demographic composition; namely the issue of demographic basis risk described in Mosher and Sagoo (2011).

Starting from a given age x at initial time t, the average mortality intensities $\bar{\mu}^R_{x,t}$ and $\bar{\mu}^B_{x,t}$ of the book and reference populations are modelled as affine functions of the time-varying factors

$$\begin{aligned}\bar{\mu}^R_{x,t} &= \delta_{R,0} + \delta_{R,1} C_{x,t} + \delta_{R,2} R_{x,t},\\ \bar{\mu}^B_{x,t} &= \delta_{B,0} + \delta_{B,1} C_{x,t} + \delta_{B,2} B_{x,t}.\end{aligned}$$

The factors are assumed to evolve independently, implying that the common factor does not depend on the local factors. This allows the joint ATSM to be decomposed into two single-population term structure mortality models (Egorov et al., 2011). Due to the incompleteness of the longevity market, Xu et al. (2019) define a best-estimate measure $\bar{Q}$, fixed to observed mortality rates. Factor dynamics under $\bar{Q}$ can be represented as

$$\begin{bmatrix} dC_{x,t} \\ dR_{x,t} \\ dB_{x,t} \end{bmatrix} = - \begin{bmatrix} \phi_1 & 0 & 0 \\ 0 & \phi_2 & 0 \\ 0 & 0 & \phi_3 \end{bmatrix} \begin{bmatrix} C_{x,t} \\ R_{x,t} \\ B_{x,t} \end{bmatrix} dt + \begin{bmatrix} \sigma_1 & 0 & 0 \\ 0 & \sigma_2 & 0 \\ 0 & 0 & \sigma_3 \end{bmatrix} \begin{bmatrix} dW_t^{\bar{Q},C} \\ dW_t^{\bar{Q},R} \\ dW_t^{\bar{Q},B} \end{bmatrix},$$

where ϕ_1, ϕ_2, ϕ_3, σ_1, σ_2 and σ_3 are constant parameters with $W_t^{\bar{Q},C}$, $W_t^{\bar{Q},R}$ and $W_t^{\bar{Q},B}$ being Wiener processes under the best-estimate measure.

In order to derive the factor dynamics under the real-world probability measure, P, we use Girsanov's theorem (Girsanov, 1960) to relate the best-estimate Wiener process to their real-world counterparties. Using an essentially affine risk premium specification, the change of measure can be described as follows

$$\begin{bmatrix} dW_t^{\bar{Q},C} \\ dW_t^{\bar{Q},R} \\ dW_t^{\bar{Q},B} \end{bmatrix} = \begin{bmatrix} dW_t^{P,C} \\ dW_t^{P,R} \\ dW_t^{P,B} \end{bmatrix} + \left[\begin{bmatrix} \gamma_1^0 \\ \gamma_2^0 \\ \gamma_3^0 \end{bmatrix} + \begin{bmatrix} \gamma_{1,1}^1 & \gamma_{1,2}^1 & \gamma_{1,3}^1 \\ \gamma_{2,1}^1 & \gamma_{2,2}^1 & \gamma_{3,3}^1 \\ \gamma_{3,1}^1 & \gamma_{3,2}^1 & \gamma_{3,3}^1 \end{bmatrix} \begin{bmatrix} dC_{x,t} \\ dR_{x,t} \\ dB_{x,t} \end{bmatrix} \right] dt, \tag{1}$$

where the γ parameters are constant and $W_t^{P,C}$, $W_t^{P,R}$ and $W_t^{P,B}$ are Brownian motions under the real-world measure. Substituting the vector of best-estimate Wiener processes into equation (1) and assigning values to the γ parameters as appropriate, the real world dynamics can be expressed as

$$\begin{bmatrix} dC_{x,t} \\ dR_{x,t} \\ dB_{x,t} \end{bmatrix} = - \begin{bmatrix} \psi_1 & 0 & 0 \\ 0 & \psi_2 & 0 \\ 0 & 0 & \psi_3 \end{bmatrix} \begin{bmatrix} C_{x,t} \\ R_{x,t} \\ B_{x,t} \end{bmatrix} dt + \begin{bmatrix} \sigma_1 & 0 & 0 \\ 0 & \sigma_2 & 0 \\ 0 & 0 & \sigma_3 \end{bmatrix} \begin{bmatrix} dW_t^{P,C} \\ dW_t^{P,R} \\ dW_t^{P,B} \end{bmatrix},$$

where ψ_1, ψ_2 and ψ_3 are constant parameters. We use the real-world measure to model observed mortality dynamics across the two populations and to simulate future factor paths.

Taking a conditional expectation with respect to the best-estimate probability measure, Xu et al. (2019) show that survival probabilities for the reference and book populations are respectively given by

$$\begin{aligned} S^R(x,t,T) &= e^{B_1(t,T)C_{x,t} + B_2(t,T)R_{x,t} + A^R(t,T)}, \\ S^B(x,t,T) &= e^{B_1(t,T)C_{x,t} + B_3(t,T)B_{x,t} + A^B(t,T)}, \end{aligned}$$

where

$$B_j(t,T) = -\frac{1 - e^{-\phi_j(T-t)}}{\phi_j} \qquad \text{for} \quad j = 1,2,3,$$

$$A^R(t,T) = \frac{1}{2} \sum_{j=1,2} \frac{\sigma_j^2}{\phi_j^3} [\frac{1}{2}(1 - e^{-2\phi_j(T-t)}) - 2(1 - e^{-\phi_j(T-t)}) + \phi_j(T-t)],$$

$$A^B(t,T) = \frac{1}{2} \sum_{j=1,3} \frac{\sigma_j^2}{\phi_j^3} [\frac{1}{2}(1 - e^{-2\phi_j(T-t)}) - 2(1 - e^{-\phi_j(T-t)}) + \phi_j(T-t)].$$

The average force of mortality curve for each population is modelled as

$$\begin{aligned} \bar{\mu}_{x,t}^i(T) &= -\frac{1}{T-t} \log[S^i(x,t,T)] \\ &= -\frac{1}{T-t} [B_1(t,T)C_{x,t} + B_j(t,T)i_{x,t} + A_t^i(t,T)] \\ &= \frac{1 - e^{-\phi_1(T-t)}}{\phi_1(T-t)} C_{x,t} + \frac{1 - e^{-\phi_j(T-t)}}{\phi_j(T-t)} i_{x,t} - \frac{A_t^i(t,T)}{T-t}, \text{ for } \quad i = \begin{Bmatrix} R, & (j=2) \\ B, & (j=3) \end{Bmatrix}. \end{aligned}$$

The model can be written in state space form and can therefore be estimated using the Kalman filter (Kalman, 1960). In particular, the state space form consists of a measurement equation, which specifies the relationship between the average mortality intensities

$\bar{\mu}_{x,t}$ and the factors $R_{x,t}$, $B_{x,t}$ and $C_{x,t}$, as well as a state transition equation which describes the time series dynamics of the latent time-varying factors. These equations are presented in Appendix A.

We define the reference population to be the US national male population and the book population as a pool of lifetime income stream income recipients whose mortality reflects that of an affluent subset of the US male population. As with Xu et al. (2019) and Luciano et al. (2017), we choose male mortality in order to establish upper bounds on the market price of longevity risk.

For the reference population mortality evolution, we use single-year single-age population-level deaths and exposure data for US males from ages 65 to 99 between 1980 and 2015 sourced from the Human Mortality Database (2018)[6]. A starting year of 1980 is selected to reflect the period analysed in Li et al. (2017) who highlight the structural differences in mortality in prior periods noted by various authors (Renshaw and Haberman, 2003; Li and Hardy, 2011).

However, time series deaths and exposure data for US annuity holders is not publicly available. Therefore, we construct a synthetic book population which is assumed to approximate the demographics of a typical retirement income portfolio. The United States Mortality Database (2018)[7] publishes state-level mortality data over the period 1959 to 2015. We aggregate the exposure and deaths data using the set of states in the highest US income quintile based on state-level average household income statistics published in Small Area Income and Poverty Estimates Program (2018)[8] in order to construct a synthetic book population mortality dataset of single-year single-age deaths and exposure data from ages 65 to 99 between 1980 and 2015. This methodology is underpinned by the assumption that retirement income portfolios typically consist of more affluent subsets of the population (Coughlan et al., 2011).

The average force of mortality for the reference and book populations over the in-sample period is shown in Figures 2(a) and 2(b), respectively. Both populations clearly exhibit mortality improvement over time. The book population generally has lower mortality relative to the reference population, a feature which is highlighted when comparing initial mortality rates for selected ages across the two populations as depicted in Figures 2(c) and 2(d).

The model can be estimated using the Kalman filter (Kalman, 1960) which employs maximum likelihood estimation techniques to calibrate model parameters by simultaneously fitting the observed average force of mortality to the model average force of mortality for each population. Having estimated the model parameters, we then forecast and simulate the future average force of mortality and the associated survival probabilities starting from age x over N years, where N is the initial horizon of the annuity liability. The forecasting of survival probabilities is achieved as follows:

1. Forecast the common, reference and book factors $C^F_{x,t}$, $R^F_{x,t}$, $B^F_{x,t}$ for years $t = 1, 2, ..., N$ from the estimated joint ATSM starting from age x.

2. Substitute the forecast factors into the average force of mortality functions to fore-

[6] www.mortality.org/

[7] https://usa.mortality.org/

[8] https://www.census.gov/en.html

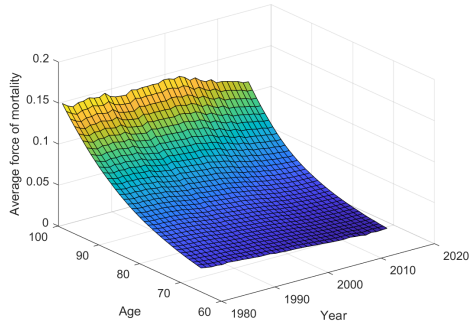

(a) Reference average mortality intensity

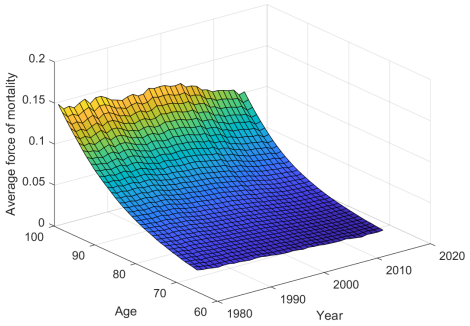

(b) Book average force of mortality

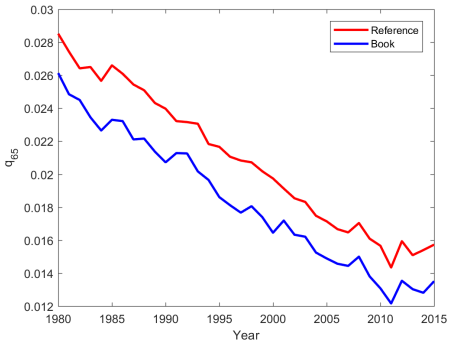

(c) Age 65 initial mortality rates

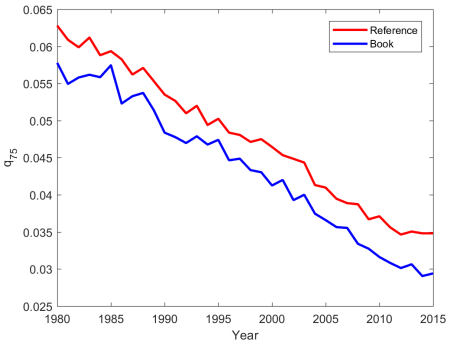

(d) Age 75 initial mortality rates

Figure 2: Observed mortality for ages 65 to 99 from 1980 to 2015 in the reference and book populations for US males showing mortality improvement across both populations and lower mortality in the book population.

cast the average force of mortality starting from age x

$$\bar{\mu}^{i,F}_{x,t}(T) = \frac{1-e^{-\phi_1(T-t)}}{\phi_1(T-t)}C^F_{x,t} + \frac{1-e^{-\phi_j(T-t)}}{\phi_j(T-t)}i^F_{x,t} - \frac{A^i_t(t,T)}{T-t} \text{ for } \quad i = \begin{Bmatrix} R, \ (j=2) \\ B, \ (j=3) \end{Bmatrix}.$$

3. Compute the associated survival probability forecasts

$$S^{R,F}(x,t,T) = e^{(-\bar{\mu}^{R,F}_{x,t}(T)\times(T-t))},$$
$$S^{B,F}(x,t,T) = e^{(-\bar{\mu}^{B,F}_{x,t}(T)\times(T-t))}.$$

The simulation of survival probabilities follows a similar procedure, using the simulated factors in place of the forecast factors. We simulate a large number of factor paths and the corresponding survival probabilities matching the liability horizon.

In addition to the continuous-time affine framework, we also fit a discrete-time multi-population mortality model for validation purposes. Drawing on the methodology developed by the LBRWG (Haberman et al., 2014; Villegas et al., 2017; Li et al., 2017, 2019), the M7-M5 model is adopted. This model allows for inter-age mortality correlations and is appropriate for basis risk assessments for annuity portfolios that have at least 25,000 lives, 8 years of reliable data, a stable demographic mix and do not have book specific cohort effects. The specification, calibration and forecasting of the M7-M5 model are detailed in Appendix B.

2.2 Interest Rate Modelling Framework

Apart from uncertainty in future mortality rates, the value of longevity-linked liabilities is also significantly impacted by financial risk; hedging analyses that fail to incorporate uncertainty associated with interest rates cannot support the credible evaluation of index-based swaps for the purposes of hedging retirement income portfolio risk exposures. We adopt the dynamic Nelson-Siegel (DNS) interest rate model with independent factors, as developed in Diebold and Li (2006), to model financial risk. Belonging to the affine term structure class of interest rate models, the DNS model is mathematically tractable and has closed-form zero-coupon bond prices.

The development of the DNS model originates from the yield curve function pioneered in Nelson and Siegel (1987). However, it models bond yields as a function of latent time-varying factors, thus allowing yields of any maturity to be forecast or simulated over any given horizon. Diebold and Li (2006) also show that this model provides good empirical fit. We fit the DNS model to both nominal (N) and real (R) interest rate data, adopting the conventional assumption of independence between mortality dynamics and interest rates (Biffis, 2005). The nominal interest rate model is required for the discounting of index swap payments, while the real interest rate model facilitates the valuation of inflation-linked liabilities. No dependence between the two interest rate processes is modelled. This assumption is underpinned by the Fisher effect which posits that real interest rates are independent of monetary measures such as nominal interest rates; a hypothesis which has been supported by numerous recent empirical studies (Panopoulou and Pantelidis, 2016; Uribe, 2018; Cai, 2018).

Beginning with the nominal interest rate model, we first define the three latent time-varying factors: a level factor L^N_t, a slope factor S^N_t and a curvature factor C^N_t. As the

independent-factor DNS model is not constrained to a unique specification of the factor dynamics under the real-world probability measure (Christensen et al., 2011), we initially present the risk-neutral Q dynamics of the factors. The risk-neutral measure supports the valuation of future cashflows and has the following factor dynamic specification under our modelling framework

$$\begin{bmatrix} dL_t^N \\ dS_t^N \\ dC_t^N \end{bmatrix} = - \begin{bmatrix} 0 & 0 & 0 \\ 0 & \lambda^N & -\lambda^N \\ 0 & 0 & \lambda^N \end{bmatrix} \begin{bmatrix} L_t^N \\ S_t^N \\ C_t^N \end{bmatrix} dt + \begin{bmatrix} \sigma_1^N & 0 & 0 \\ 0 & \sigma_2^N & 0 \\ 0 & 0 & \sigma_3^N \end{bmatrix} \begin{bmatrix} dW_t^{Q,L^N} \\ dW_t^{Q,S^N} \\ dW_t^{Q,C^N} \end{bmatrix},$$

where λ^N is the Nelson-Siegel parameter, σ_1^N, σ_2^N and σ_3^N are the factor volatility parameters, while W_t^{Q,L^N}, W_t^{Q,S^N} and W_t^{Q,C^N} are the corresponding Wiener processes.

We use the real-world measure to model observed bond yield data and to simulate future factor paths. However, Christensen et al. (2011) note that in order to maintain affine dynamics under the real world probability measure, an essentially-affine risk premium specification must be assumed upon invoking the Girsanov theorem (Girsanov, 1960) when changing the measure from Q to P. Therefore, the real-world factor dynamics are represented as

$$\begin{bmatrix} dL_t^N \\ dS_t^N \\ dC_t^N \end{bmatrix} = \begin{bmatrix} k_1^N & 0 & 0 \\ 0 & k_2^N & 0 \\ 0 & 0 & k_3^N \end{bmatrix} \left[\begin{bmatrix} \theta_{1,N} \\ \theta_{2,N} \\ \theta_{3,N} \end{bmatrix} - \begin{bmatrix} L_t^N \\ S_t^N \\ C_t^N \end{bmatrix} \right] dt + \begin{bmatrix} \sigma_1^N & 0 & 0 \\ 0 & \sigma_2^N & 0 \\ 0 & 0 & \sigma_3^N \end{bmatrix} \begin{bmatrix} dW_t^{P,L^N} \\ dW_t^{P,S^N} \\ dW_t^{P,C^N} \end{bmatrix},$$

where k_1^N, k_2^N, k_3^N, θ_1^N, θ_2^N and θ_3^N are constant real-world parameters, W_t^{P,L^N}, W_t^{P,S^N} and W_t^{P,C^N} are Wiener processes under the P measure.

Given the model dynamics under the risk neutral measure, the zero coupon nominal bond yield at time t with τ months maturity is given by the yield function

$$y_t^N(\tau) = L_t^N + S_t^N \left(\frac{1 - e^{-\lambda^N \tau}}{\lambda^N \tau} \right) + C_t^N \left(\frac{1 - e^{-\lambda^N \tau}}{\lambda^N \tau} - e^{-\lambda^N \tau} \right).$$

For the nominal yield data, we use monthly observations published by the US Department of the Treasury[9] from October 2006 to May 2018 as this provides complete data across all eleven published maturity terms: 1 month, 3 months, 6 months, 1 year, 2 years, 3 years, 5 years, 7 years, 10 years, 20 years and 30 years. The summary statistics for the empirical nominal yield rates are provided in Table 1.

The empirical data is presented in Figure 3(a). In general, the yield curve is upward-sloping with respect to maturity over the in-sample period. We also note higher volatility in the short-term interest rates relative to the long-term rates. Indeed, the standard deviation of 1 month yields is almost double the mean.

As with the joint ATSM, the DNS interest rate model can be expressed in state space form in terms of a measurement equation and a state transition equation as detailed in Appendix C. Therefore, it can be estimated using the Kalman filter (Kalman, 1960). We

[9] `https://home.treasury.gov/`

Maturity (months)	Mean	Standard Deviation	Min	Max
1	0.98	1.63	0.00	5.24
3	1.04	1.65	0.00	5.16
6	1.14	1.67	0.03	5.24
12	1.23	1.61	0.09	5.21
24	1.43	1.47	0.20	5.16
36	1.66	1.37	0.30	5.13
60	2.14	1.21	0.59	5.10
84	2.54	1.09	0.98	5.11
120	2.91	1.00	1.46	5.15
240	3.46	0.97	1.78	5.35
360	3.63	0.83	2.18	5.21

Table 1: Nominal US interest rate summary statistics from October 2006 to May 2018.

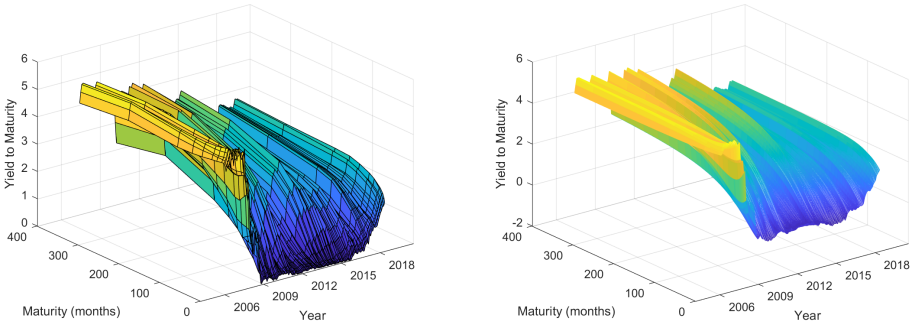

(a) Observed

(b) Fitted

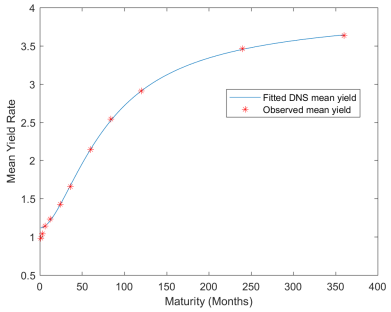

(c) Mean

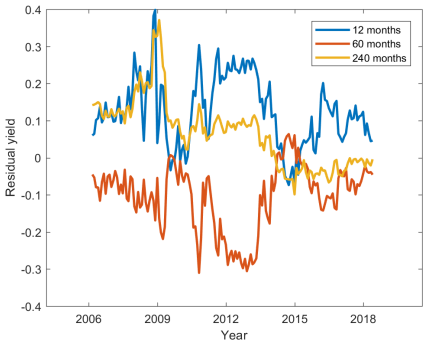

(d) Residuals

Figure 3: Nominal US bond yields from October 2006 to May 2018 indicating that key data features have been effectively captured

apply the Kalman filtering technique to the observed nominal bond yield data. The fitted yields are presented in Figure 3(b) and broadly capture the key features of the observed interest rate data. Figure 3(c) compares the empirical and fitted mean yield curves, while Figure 3(d) presents the model residuals' time series for selected maturities. These figures confirm the satisfactory overall fit of the estimated interest rate model, although fitting performance for maturities under 3 months is less precise and is more volatile, which is in line with the high relative standard deviations observed in the summary statistics at the short end of the yield curve. However, given that our basis risk analysis is based on maturities ranging from 1 year to 35 years, the model fits well over the most relevant maturities. This is confirmed by the the mean and standard deviations of the model residuals by maturity provided in Table 2. These residuals are broadly in line with those reported in Christensen et al. (2010).

Maturity (months)	Mean (bps)	Standard Deviation (bps)
1	-13.3333	6.6372
3	-7.5352	5.9266
6	0.3016	0.7937
12	2.3771	6.6486
24	0.9736	5.7837
36	-1.2565	2.5624
60	-0.1157	5.2012
84	2.1626	4.2657
120	-0.0610	0.8739
240	0.8163	4.0693
360	-1.0173	3.2993

Table 2: Nominal US interest rates: residual mean and standard deviation by maturity.

Having estimated the model, we then forecast and simulate the future term structure of interest rates and the associated zero coupon bond prices over N years. The forecasting of zero coupon bond prices is achieved as follows:

1. Forecast the level, slope and curvature factors L_t^F, S_t^F, C_t^F for years $t = 1, 2, ..., N$ from the estimated DNS interest rate model.

2. Substitute the forecast factors into the yield function to forecast the term structure of interest rates

$$y_t^F(\tau) = L_t^F + S_t^F \left(\frac{1 - e^{-\lambda\tau}}{\lambda\tau} \right) + C_t^F \left(\frac{1 - e^{-\lambda\tau}}{\lambda\tau} - e^{-\lambda\tau} \right).$$

3. Compute the associated zero coupon bond price forecasts:

$$P^F(t, T) = e^{(-y_t^F(T-t) \times (T-t))}.$$

The simulation of zero coupon bond prices follows a similar procedure, using the simulated factors in place of the forecast factors. We simulate a large sample of factor paths and corresponding bond prices over the liability horizon as in the mortality forecasting case.

The modelling of real interest rates is equivalent to that of nominal rates described above. To calibrate the real DNS interest rate model, we use monthly observations published by

the US Department of the Treasury[10] from February 2010 to May 2018 as this provides complete data across all five published maturity terms: 5 years, 7 years, 10 years, 20 years and 30 years. Although it is possible to go further back, doing so necessitates excluding the 30-year maturity from the estimation set which could materially compromise the model's out-of-sample forecasting performance given our required 35-year forecasting horizon. The summary statistics for the empirical real yield rates are provided in Table 3.

Maturity (months)	Mean	Standard Deviation	Min	Max
60	-0.24	0.57	-1.47	0.72
84	0.08	0.54	-1.20	1.23
120	0.34	0.50	-0.79	1.60
240	0.81	0.46	-0.09	1.99
360	1.05	0.43	0.32	2.16

Table 3: Real US interest rate summary statistics from February 2010 to May 2018

The empirical data is shown in Figure 4(a). Similarly to the nominal interest rate data, the real yield curve also slopes upwards with respect to maturity over the in-sample period and higher volatility is observed in the short-term interest rates relative to the long-term rates. However, unlike the nominal interest rates, we observe negative bond yields at various different time points, particularly in the 5 year maturity range.

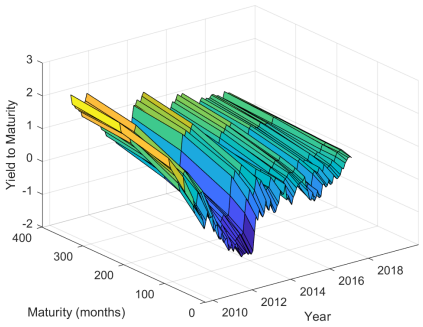

(a) Observed

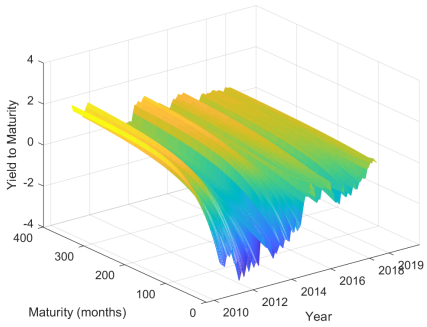

(b) Fitted

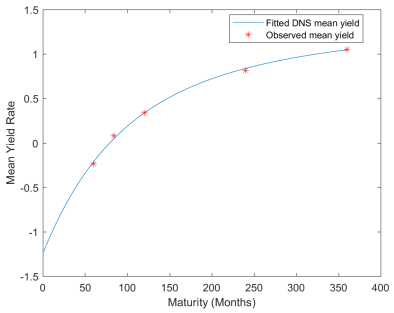

(c) Mean

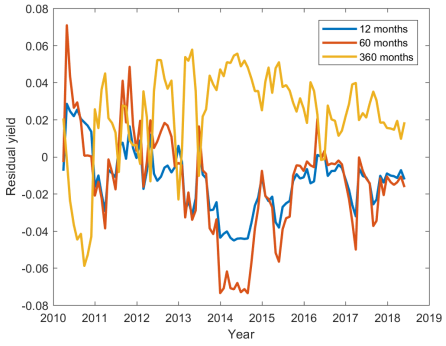

(d) Residuals

Figure 4: Real US bond yields from February 2010 to May 2018 indicating that key data features have been effectively captured

We apply the Kalman filtering technique to the observed real bond yield data. The fitted yields are presented in Figure 4(b) and broadly capture the key features of the observed

[10] `https://home.treasury.gov/`

interest rate data. Figure 4(c) compares the empirical and fitted mean yield curves, while Figure 4(d) presents the model residuals for selected maturities. These figures confirm the satisfactory overall fit of the estimated interest rate model. This is confirmed by the the mean and standard deviations of the model residuals by maturity provided in Table 4. These residuals are broadly in line with those reported in Xu et al. (2019). The forecasting and simulation of real zero coupon bond yields and prices reflects the framework described previously for the nominal interest rates.

Maturity (months)	Mean (bps)	Standard Deviation (bps)
60	-2.4091	5.6250
84	3.1164	6.7812
120	0.0000	0.0000
240	-2.3681	3.3248
360	0.3077	0.8901

Table 4: Real US interest rates: residual mean and standard deviation by maturity.

3 Liability Profile

For our hedging analysis, we assume that a retirement income provider is aiming to hedge the risks associated with a closed annuity pool comprising of individuals from a single cohort initially aged x in year t who are promised \$1 of inflation-indexed income per year upon survival from ages $x+1$ to the maximum attainable age, ω, hence the initial horizon of the annuity liability is given by $\omega - x$. The present value of the retirement income portfolio liability is

$$PV(\text{Unhedged Portfolio}) = \sum_{i=1}^{\omega-x} l^B_{x+i,t+i} \times P_R(t, t+i),$$

where $l^B_{x+i,t+i}$ is the number of surviving annuitants (aged $x+i$ at time $t+i$) and this is dependent on the simulated book population mortality dynamics generated by the chosen mortality model. However, we also account for sampling basis risk by allowing the number of deaths in any given year to follow a binomial distribution $D^B_{x,t} \sim \text{Bin}(E^B_{x,t}, q^B_{x,t})$ (Haberman et al., 2014) where the exposure $E^B_{x,t}$ is given by the number of surviving annuitants in year t and the mortality rate parameter $q^B_{x,t}$ is simulated from the mortality model. The quantity, $P_R(t, t+i)$, is the time t price of an inflation-indexed zero coupon bond making a single unit payment at time $t+i$ as computed from the real interest rate model.

In Figure 5, we plot a histogram showing 10,000 simulations of the liability present value for a portfolio with an initial size of 100,000 lives based on a starting age of $x = 65$ and an assumed final payment age of $\omega = 100$, giving an initial liability term of $\omega - x = 35$ years. A degree of positive skewness is apparent, with the simulated distribution exhibiting a heavier right tail. This highlights the importance of effectively hedging against more extreme outcomes in pension liabilities resulting from unexpected mortality or financial market experience.

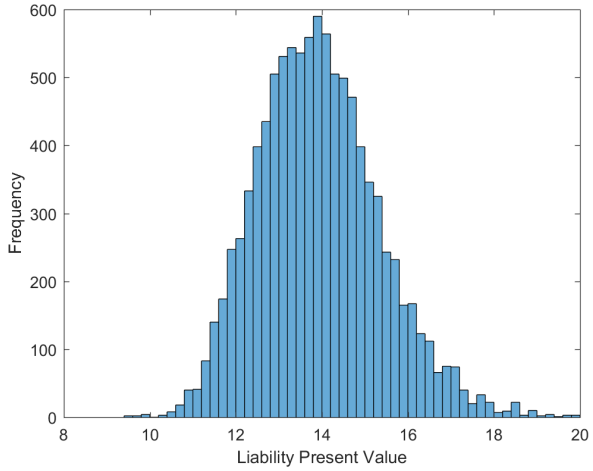

Figure 5: Liability present value histogram for the book population cohort initially aged 65 (joint ATSM, 10,000 simulations, 100,000 lives).

4 Value-Based Longevity Index Computation

As presented in Section 2, we define the value-based longevity index, $I_{x,t}$, as the expected present value of a unit of longevity and inflation-indexed income paid annually in arrears to a cohort aged x at initial time t. Drawing on the survival probabilities of the reference population, as generated by the continuous-time mortality model, as well as forecast real zero coupon bond prices, we compute the initial (that is, time $t = 0$) index values for ages 65 to 99, as depicted in Figure 6. The index value for age 65 is 12.98, that is, for each 65 year old male who is promised \$1 of inflation-indexed income per year upon survival from ages 66 to 100, a retirement income provider requires \$12.98 worth of investments today.

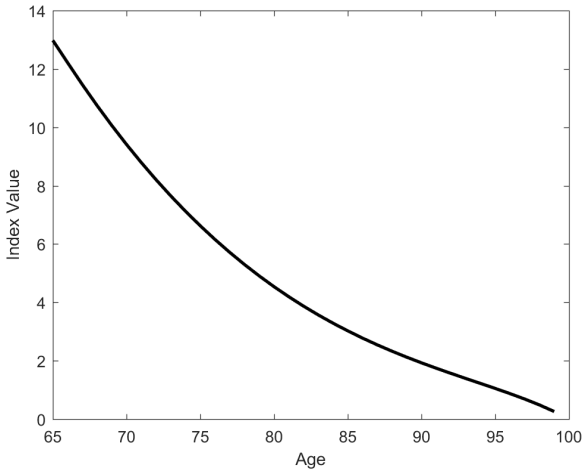

Figure 6: Initial index value by age from 65 to the maximum attainable age, $\omega = 100$.

It is also possible to forecast and simulate future index values over time based on mortality and interest rate forecasts and simulations. For example, the forward index values for the cohort initially aged $x = 65$ (at time $t = 0$) is represented by the black curve in Figure 7. This shows the expected path of the value-based longevity index over the payment period for this particular reference population cohort, where a smooth and stable decline is observed.

In reality, mortality, interest rate and inflation factors will differ over time from initial forecasts and hence the evolution of the index will not exactly track its expected pathway. Figure 7 also shows 10,000 simulations of the index value for the cohort initially aged $x = 65$. We note that although the forward index values remain broadly in the middle of the distribution of simulated paths, there is material variability around the expected value over time. The volatility around the forward values declines over time until the final age is reached.

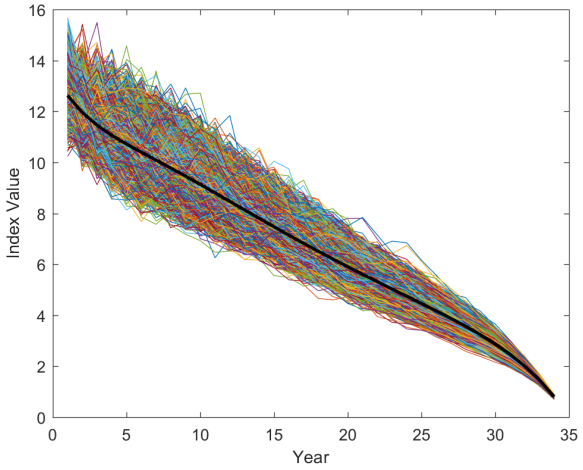

Figure 7: Forward and simulated index values for the reference population cohort initially aged 65 (joint ATSM, 10,000 simulations).

5 The Hedging Framework

Assume that an annually-settled index swap trades in the longevity risk transfer market. For a given age x at initial time t, the swap references the constructed value-based longevity index $I_{x,t}$; at time $t+i$, the fixed leg pays the i year forward index value $I^f_{x+i,t+i}$ while the floating leg pays the realised index value $I_{x+i,t+i}$. As index values are based on forward-looking cashflows, the final swap payment is made when the initial cohort reaches age $\omega - 1$; not at age ω when the final annuity payments are made to surviving policyholders. That is, the swap has an initial maturity term of $\omega - x - 1$, hence the longevity, interest rate and inflation risk over the final year of the liability remain unhedged. This mismatch between liability and hedge cashflows constitutes an example of structuring basis risk.

A retirement income provider seeking to hedge their risk exposure would be the fixed leg payer to this index swap. From their perspective, the random present value of the swap instrument is

$$PV(\text{Index Swap}) = \sum_{i=1}^{\omega-x-1} (I_{x+i,t+i} - I^f_{x+i,t+i}) \times P_N(t, t+i),$$

where $x = 65$ and $\omega = 100$, $I^f_{x+i,t+i}$ denotes the forward index value which is computed from central forecasts, and $I_{x+i,t+i}$ denotes the realised index value whose computation entails two distinct steps. The initial phase involves the simulation of a single mortality

intensity and interest rate path up until time $t+i$. In the second stage, conditional on the mortality and interest rate realisations in the first phase, central forecasts from time $t+i$ onwards are computed to derive the realised index value $I_{x+i,t+i}$. The quantity, $P_N(t, t+i)$, is the time t price of a nominal zero coupon bond making a single unit payment at time $t+i$, and this is simulated from the nominal interest rate model.

For an index swap written on the index for the cohort initially aged $x = 65$, the simulated swap payment paths received by the fixed leg payer over the $\omega - x - 1 = 34$-year swap term is shown in Figure 8. These swap simply represent the difference between the simulated and forward index values over time shown in Figure 7.

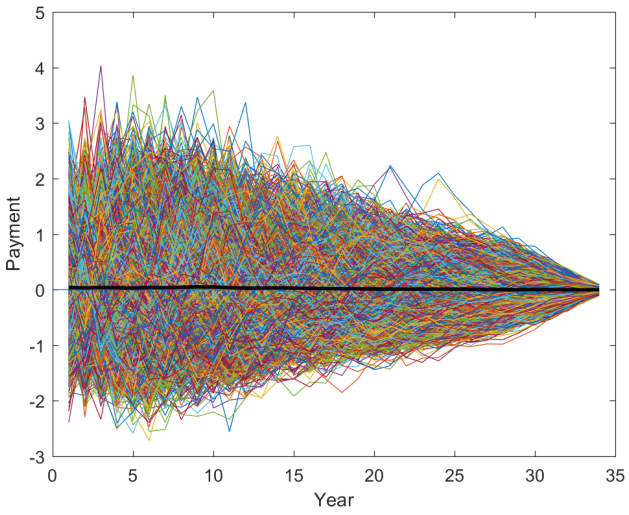

Figure 8: Simulated swap payments for the reference population cohort initially aged 65 (joint ATSM, 10,000 simulations).

Although individual swap payment paths can be volatile, the average swap payment as depicted by the black line remains very close to zero. This reflects the fact that forward index values are simply assumed to follow the expected values with no risk or profit premiums priced in to the forward values. As reflected in Figure 7, the variability of swap payments is highest in the early years of the hedge and steadily decreases over the term of the swap. This is because the earlier that unexpected deviations in experience occur, the greater the number of remaining future cashflows to be impacted, and hence the expected present value of future cashflows is more sensitive in the early years to emerging unexpected deviations in mortality, inflation and interest rate experience.

When retirement income providers hedge their exposure using the swap instrument, they effectively combine the hedging instrument with their exposed portfolio. Therefore, the random present value of the retirement income providers' hedged portfolio is given by the sum of the the present values of the two components

$$\begin{aligned} &PV(\text{Hedged Portfolio}) = PV(\text{Unhedged Portfolio}) + PV(\text{Index Swap}) \\ &= \sum_{i=1}^{\omega-x} l^B_{x+i,t+i} \times P_R(t, t+i) + w_0 \sum_{i=1}^{\omega-x-1} (I_{x+i,t+i} - I^f_{x+i,t+i}) \times P_N(t, t+i), \end{aligned}$$

where w_0 refers to the notional amount of the longevity swap. As with Li et al. (2017), w_0 is estimated using numerical optimisation with an objective to minimise the variance of

the hedged portfolio's present value (Appendix D) conditional on the simulated liability values and realised swap payment paths, obtaining a solution of $w_0 = 0.3056$.

6 Basis Risk Metrics

Inspired by Chang and Sherris (2018), we compare the hedge outcomes associated with the value-based longevity index to two other longevity indices which we also construct. The purpose of these comparisons is to attribute the risks associated with retirement income portfolios into longevity risk, interest rate risk and inflation risk components.

We define the index $I^0_{x,t}$ as the expected survival probability of a cohort aged x in year t. The survival index value is represented as

$$I^0_{x,t} = \sum_{i=1}^{\omega-x} S^R(x, t, t+i),$$

where $S^R(x, t, t+i)$ denotes the forecast i year survival probability of the reference population.

We define the index $I^1_{x,t}$ as the expected present value of a unit of longevity-indexed income paid annually in arrears to a cohort aged x in year t. The index value is represented as

$$I^1_{x,t} = \sum_{i=1}^{\omega-x} S^R(x, t, t+i) \times P_N(t, t+i),$$

where $S^R(x, t, t+i)$ denotes the forecast i year survival probability of the reference population and $P_N(t, t+i)$ is the forecast time t price of a nominal zero coupon bond making a single unit payment at time $t+i$ as computed from the nominal interest rate model.

The attribution of risk can be outlined as follows:

- The risk reduction achieved by hedging the retirement income portfolio using $I^0_{x,t}$ as the reference index represents the impact of longevity risk.
- The additional risk reduction achieved by hedging the retirement income portfolio using $I^1_{x,t}$ as the reference index (relative to a hedge referencing the index $I^0_{x,t}$) represents the impact of interest rate risk.
- The additional risk reduction achieved by hedging the retirement income portfolio using $I_{x,t}$ as the reference index (relative to a hedge referencing the index $I^1_{x,t}$) represents the impact of inflation risk.

Having calibrated the longevity swap instrument, it is critical to assess the effectiveness of the hedging strategy. We initially adopt graphical risk reduction representations as visualisation can be a very efficient way to communicate the effectiveness of hedging strategies to a variety of different stakeholders. Following Coughlan (2009), we plot the simulated liability distributions to obtain a preliminary overview of the degree of risk reduction achieved by the index-based hedge, as well as the other comparison indices described above.

In Figure 9, the blue histograms represent the present value of the *unhedged* portfolio liability outcomes, while the overlaid orange histograms represent the net present value of the *hedged* liability outcomes (that is, the sum of the unhedged liability outcomes and the weighted index swap outcomes). These diagrams represent annuity pools with 100,000 initial members. For all three indices, we observe a reduction in the volatility of liability valuations once the index swaps have been taken into account. However, as depicted in Figure 9(c), it is also apparent that when the liability is hedged with reference to the inflation-indexed value-based longevity index $I_{x,t}$, the hedged distribution becomes materially narrower relative to the two alternate longevity indices.

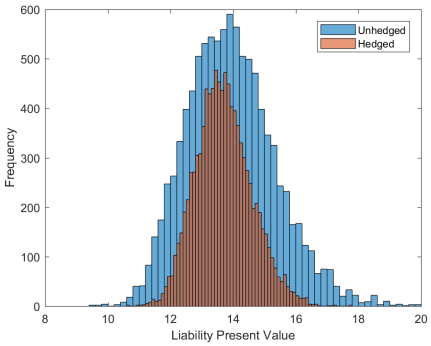

(a) Survival index $I^0_{x,t}$

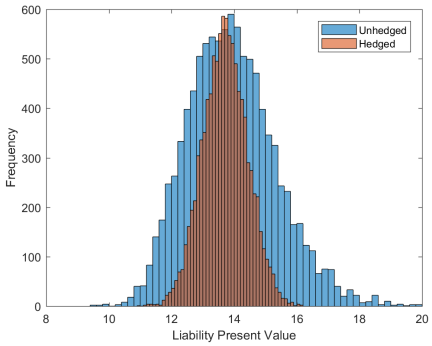

(b) Nominal-linked value index $I^1_{x,t}$

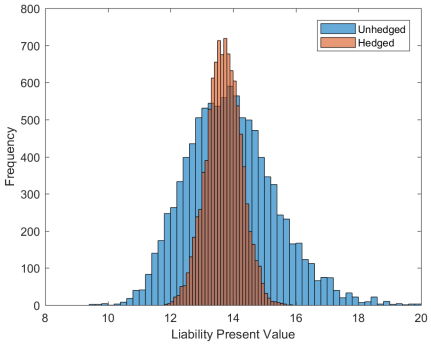

(c) Inflation-linked value index $I_{x,t}$

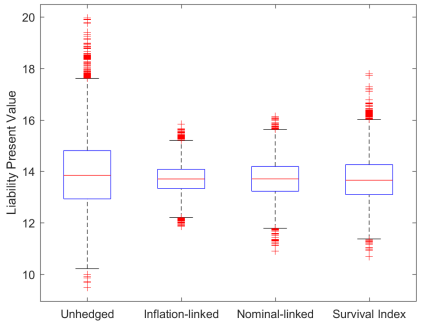

(d) Box and whisker plots of the liability present value distribution by hedging index

Figure 9: Hedged and unhedged liability present value distributions by hedging index (joint ATSM, 10,000 simulations, 100,000 lives).

We also present a box and whisker plot of the simulated liability present value outcomes in Figure 9(d). In all four simulated distributions, the median outcome as indicated by the central mark is relatively similar. However, once we examine the 25^{th} and 75^{th} percentiles of the liability distribution (represented by the lower and upper edges of the box respectively), we note that variability is materially reduced when comparing the inflation-linked hedge against the unhedged liability as well as the two other alternate hedging indices. Furthermore, the outliers associated with the simulated net liability outcomes (indicated by the red crosses) are much less extreme in the case of the inflation-linked value-based longevity index, confirming the observations inferred from the histograms in Figure 9.

However, although graphical representations can provide an adequate understanding of hedging efficiency, in order to systematically evaluate the hedge effectiveness of the inflation-indexed value-based longevity index relative to the other longevity indices, quantitative

risk measures must also be examined. Therefore, we investigate the summary statistics of the simulated liability present value distributions, as presented in Table 5. From these figures, it is evident that the minimum and maximum outcomes are much less extreme and the variance of the liability present value distribution is materially reduced by hedging. Indeed, given the approximate normality of the distributions observed in Figure 9, we conduct an F-test for equality of two variances to formally examine whether the variance of the liability present value is reduced when hedged against the inflation-linked value index relative to the two other indices. Against a one-sided alternative, we are able to reject the null hypothesis at all reasonable significance levels (p-value < 0.0001) and conclude that the variance of the hedged liability tied to the inflation-linked value index is lower than the other indices at a statistically-significant level.

Hedging Index	Minimum	Maximum	Mean	Variance
Unhedged	9.47	19.97	13.92	2.00
Survival index $I^0_{x,t}$	10.66	17.84	13.87	0.83
Nominal-linked value index $I^1_{x,t}$	10.87	16.13	13.87	0.52
Inflation-linked value index $I_{x,t}$	11.88	15.85	13.86	0.31

Table 5: Summary statistics: hedged and unhedged liability present value outcomes by hedging index (joint ATSM, 10,000 simulations, 100,000 lives)

The Longevity Risk Reduction (LRR) metric is also well established in the literature as a robust indicator of hedging performance for longevity-linked instruments (Coughlan et al., 2011; Li et al., 2017). Note that some authors refer to the LRR metric using alternate terms such as "hedge efficiency" (Chang and Sherris, 2018). Following Cairns et al. (2014), we define our LRR measure based on the percentage reduction in variance of the liability present value:

$$\text{Longevity Risk Reduction} = \left(-\frac{\text{var(Hedged Portfolio)}}{\text{var(Unhedged Portfolio)}}\right) \times 100\%,$$

where var(Unhedged Portfolio) and var(Hedged Portfolio) refer to the variance of the retirement income provider's net position before and after the hedge has been applied, respectively.

In Table 6, we show the LRR attained by the various indices across three different book sizes. It is apparent that all indices are ineffective at book sizes of 1,000 policyholders due to sampling basis risk. Once the portfolio size increases to 10,000 and eventually 100,000 policyholders, all three indices exhibit a much improved hedging performance. However, the LRR associated with the inflation-linked value-based longevity index remains materially superior to the other indices at all book sizes, with the magnitude of the out-performance found to be higher in larger portfolios. However, it should be noted that even in a particularly large portfolio of 100,000 annuitants, the inflation-indexed value-based longevity index does not provide a perfect hedge (LRR of 84.58%). Demographic basis risk remains a factor, while the structuring basis risk associated with the final year of the liability remaining unhedged also impacts the outcome.

The differences between the hedging outcomes associated with the three indices also provide an indication as to the relative impact of the three identified risk sources. For example, the additional risk reduction attained using the inflation-linked value index as opposed to the value index linked to nominal interest rates is over 10% in a book of 100,000 policyholders. Therefore, when hedging annuity exposures where payments are

Hedging Index	Book Size		
	1,000	10,000	100,000
Survival index $I^0_{x,t}$	31.52	54.07	58.71
Nominal-linked value index $I^1_{x,t}$	37.82	67.24	74.07
Inflation-linked value index $I_{x,t}$	42.67	77.43	84.58

Table 6: Longevity risk reduction: percentage reduction in variance showing the greater effectiveness of the inflation-linked value-based longevity index relative to alternate indices (joint ATSM, 10,000 simulations).

tied to price levels, an index that reflects the inflation-linked nature of these obligations provides a material advantage over indices that fail to account for inflation. Similarly, we observe a difference of almost 26% between the inflation-linked value index and the standard survival rate index, suggesting that retirement income providers who pursue survivor swaps when hedging inflation-linked liabilities would experience significant basis risk due to the inability of survival indices to account for inflation or interest rate risk.

7 Sensitivity Analysis

From a practitioner's perspective, it is critical to assess the significance of various modelling assumptions and experimental design settings. Following the template of Li et al. (2017), we perform robustness checks on various aspects of the modelling framework and methodological process to examine the potential impact of different assumption settings on hedge outcomes. In each of the following cases, one key experimental variable is changed, while all other factors and settings are held constant.

It is well established in the literature that the effectiveness of index-based longevity hedges are greater for larger book sizes (Villegas et al., 2017; Li et al., 2017; Chang and Sherris, 2018); a finding which is also evidenced in our analysis. It occurs because in larger retirement income portfolios, sampling basis risk lacks the sufficient leverage to materially impact aggregate hedge outcomes. To more closely examine the relationship between portfolio size and longevity risk reduction, we test our hedging framework utilising the inflation-linked value-based longevity index in portfolio sizes of 1,000; 5,000; 10,000; 25,000; 50,000 and 100,000 lives. The LRR outcomes attained at these book sizes are plotted in Figure 10.

While hedge efficiency improves at a significant rate up until about 10,000 lives, the impact of sampling basis risk on portfolio hedging outcomes becomes progressively smaller for larger pension pools, with minimal marginal benefits extracted when increasing the book size beyond 50,000 lives.

In order to evaluate the potential impact of model risk on hedging outcomes, we repeat our analysis using the simulation and forecasting results generated by the discrete-time M7-M5 mortality model (Haberman et al., 2014). This facilitates the comparison of the two mortality modelling frameworks and bridges the literature gap between continuous-time and discrete-time multi-population mortality modelling techniques. As in the previously presented example, we assume that a retirement income provider is aiming to hedge the risks associated with a pool of 65 year old males who are promised \$1 of inflation-indexed income per year upon survival from ages 66 to 100. In this analysis, the simulated interest

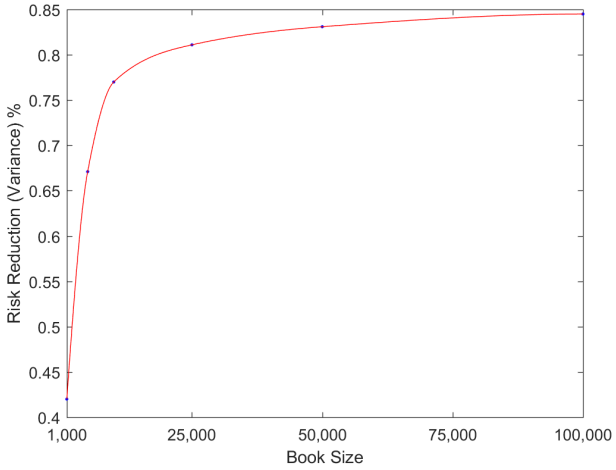

Figure 10: Hedge efficiency by book size indicating the diminishing marginal benefit of increasing book size (joint ATSM, 10,000 simulations).

rate paths are controlled from the results presented for the continuous-time analysis.

From the LRR metrics presented in Table 8 and the summary statistics detailed in Table 7, we do not observe material difference between the continuous and discrete-time mortality modelling frameworks in the analysis of hedge effectiveness. For the inflation-linked value-based longevity index, the observed LRR metric is 85.51% for a portfolio size of 100,000 with an associated swap weight parameter of $w_0 = 0.3093$. This is highly comparable to the corresponding values of 84.58% and $w_0 = 0.3056$ from the joint ATSM, with minor differences between the two approaches potentially resulting from the discretisation errors associated with the discrete-time framework.

Hedging Index	Minimum	Maximum	Mean	Variance
Unhedged	9.51	20.03	14.01	2.03
Survival index $I^0_{x,t}$	10.59	17.72	13.99	0.81
Nominal-linked value index $I^1_{x,t}$	11.24	16.37	13.97	0.51
Inflation-linked value index $I_{x,t}$	11.76	15.72	13.98	0.29

Table 7: Summary statistics: hedged and unhedged liability present value outcomes by hedging index (M7-M5 model, 10,000 simulations, 100,000 lives).

Hedging Index	Book Size		
	1,000	10,000	100,000
Survival index $I^0_{x,t}$	31.77	54.93	59.90
Nominal-linked value index $I^1_{x,t}$	38.42	68.59	74.88
Inflation-linked value index $I_{x,t}$	43.07	78.23	85.51

Table 8: Longevity risk reduction: percentage reduction in variance showing the greater effectiveness of the inflation-linked value-based longevity index relative to alternate indices (M7-M5 model, 10,000 simulations).

Having estimated both the continuous-time and discrete-time mortality modelling frameworks, we can as well examine the stability of hedging outcomes when the alternate model is used to calibrate the notional swap parameter w_0. That is, we can estimate the swap weight using the discrete-time mortality model and use this weighting to compute the

hedging outcomes associated with the value-based longevity index under the continuous-time mortality framework (and vice-versa). We find that the sensitivity of risk reduction outcomes to this variation in hedge calibration method is limited. As shown in Tables 9, 10 and 11, for the continuous-time and discrete-time mortality models, the reduction in hedging efficiency is minimal when the other model is used to compute w_0; a result which is expected given the similar swap weight parameters obtained by the two different mortality modelling frameworks, suggesting that model risk is limited.

	Joint ATSM	M7-M5 model
w_0 calibrated by same model	84.58%	85.51%
w_0 calibrated by alternate model	84.27%	85.11%

Table 9: Inflation-linked value-based longevity index: model hedge effective comparison indicating similar overall outcomes across the two mortality modelling frameworks (percentage reduction in variance, 10,000 simulations, 100,000 lives).

	Joint ATSM	M7-M5 model
w_0 calibrated by same model	74.07%	74.88%
w_0 calibrated by alternate model	73.81%	74.51%

Table 10: Nominal value-based longevity index: model hedge effective comparison indicating similar overall outcomes across the two mortality modelling frameworks (percentage reduction in variance, 10,000 simulations, 100,000 lives).

	Joint ATSM	M7-M5 model
w_0 calibrated by same model	58.71%	59.90%
w_0 calibrated by alternate model	58.36%	59.58%

Table 11: Expected survival index: model hedge effective comparison indicating similar overall outcomes across the two mortality modelling frameworks (percentage reduction in variance, 10,000 simulations, 100,000 lives).

We have demonstrated that the universal value-based longevity index facilitates superior hedging outcomes relative to standard survival rate indices, such as those examined by the LBRWG. Furthermore, we have used this index to attribute the risks arising from retirement income portfolios into longevity risk, interest rate risk and inflation risk components. Finally, we have conducted a range of sensitivity analyses on the hedging results, demonstrating that our findings can vary among retirement income portfolios of differing size, but are robust across different age ranges and mortality modelling frameworks.

8 Conclusion

This paper has made threefold contributions to the literature which are motivated by the fundamental aim of supporting and accelerating the practice of index-based longevity hedging for retirement income portfolio risk exposures and establishes a framework which facilitates the establishment of a liquid market for trading longevity-linked instruments.

A value-based longevity index has been constructed whose functionality is illustrated with the aid of US economic and mortality data. This contribution demonstrates how the

market can design an index that closely tracks the value of longevity-linked liabilities; a critical requirement for the development of a viable, liquid longevity risk transfer market. Furthermore, the construction of the value-based longevity index has facilitated the attribution of risk arising from retirement income portfolios into distinct longevity risk, interest rate risk and inflation risk components.

Key aspects have been drawn from the LBRWG's longevity basis risk quantification framework to demonstrate that hedges referencing the value-based longevity index generate material reductions in basis risk relative to survivor swap instruments based on standard mortality rate indices such as the Lifemetrics Index. Indeed, the minimisation and robust quantification of longevity basis risk represents a critical element in establishing the credibility of longevity-linked securities as viable risk management instruments for retirement income providers in practice.

The third contribution is the comparison of the continuous-time multi-population mortality modelling techniques introduced by Xu et al. (2019) to the discrete-time M7-M5 multi-population mortality model (Haberman et al., 2014) advocated by the LBRWG. Despite the differing approaches developed by these authors for modelling the relationship between the mortality patterns of multiple populations, our analysis indicates that the two frameworks suggest relatively similar outcomes when hedging retirement income portfolios by means of index-based swap instruments. While, discrete-time multi-population mortality models have been more widely used in the related literature and can be more readily fitted due to not having to trial multiple combinations of initial parameter values in estimation, the continuous-time framework has the advantage of being better integrated with financial applications such as pricing and hedging, particularly when combined with affine interest rate modelling frameworks.

Ultimately by making these contributions to the literature, our research has the potential to support the transition towards index-based longevity hedging and has established a framework for facilitating objective valuation of longevity-linked instruments. This is of critical importance since index-based longevity hedging represents arguably the most realistic prospect for a viable and liquid longevity risk transfer market, given all of the complexities associated with indemnity-based longevity hedges.

The analysis in this paper is based on a static hedging framework, where the swap weight is calibrated at the outset and thereafter does not require periodic rebalancing in response to evolving financial or mortality experience. Given the structuring basis risk arising from our forward-looking longevity index over the final year of the liability's maturity, we implement the numerical optimisation hedge calibration framework proposed by the LBRWG. Under this method, each required hedge weighting is estimated with respect to a unique set of future mortality, interest rate and inflation scenarios. However, since these scenario sets must be conditionally simulated from the relevant time point onwards given the experience already observed in each individual simulation path, it is computationally much more practical to confine our analysis to static hedging strategies in which only a single initial hedge weighting is required. An alternative hedging strategy to the LBRWG's numerical optimisation framework is based on delta hedging and may be more suited to dynamic analyses as demonstrated in Luciano et al. (2017) and De Rosa et al. (2017).

Our book population is constructed from a synthetic dataset under the assumption that the aggregation of high income states sufficiently approximates the demographics of a typical retirement income portfolio. Future research that is able to utilise authentic retirement income portfolio mortality data would further enhance the credibility of index-

based longevity hedging as a viable long-term solution for the management of longevity risk. One could also consider open-ended annuity portfolios with multiple different cohorts, as well as incorporating dependence between nominal and real bond yields into the modelling framework.

Acknowledgement

The authors acknowledge financial support from the Society of Actuaries Center of Actuarial Excellence Research Grant 2017-2020: Longevity Risk: Actuarial and Predictive Models, Retirement Product Innovation, and Risk Management Strategies, support from the Australian Research Council Discovery Project: DP170102275, support from CEPAR Australian Research Council Centre of Excellence in Population Ageing Research project number CE170100005 as well as support from the Australian Prudential Regulatory Authority and the Reserve Bank of Australia.

References

Artemis. Longevity swaps and longevity risk transfer transactions. `www.artemis.bm/library/longevity_swaps_risk_transfers.html`, 2019.

P. Barrieu, H. Bensusan, N. El Karoui, C. Hillairet, S. Loisel, C. Ravanelli, and Y. Salhi. Understanding, modelling and managing longevity risk: key issues and main challenges. *Scandinavian actuarial journal*, 2012(3):203–231, 2012.

E. Biffis. Affine processes for dynamic mortality and actuarial valuations. *Insurance: Mathematics and Economics*, 37(3):443–468, 2005.

D. Blake, A. Cairns, K. Dowd, et al. Still living with mortality: the longevity risk transfer market after one decade. `https://www.actuaries.org.uk/documents/still-living-mortality-longevity-risk-transfer-market-after-one-decade`, 2018.

Y. Cai. Testing the fisher effect in the us. *Economics Bulletin*, 38:1014–1027, 2018.

A. Cairns. Basis risk in index based longevity hedges: A guide for longevity hedgers. 01 2017.

A. Cairns, K. Dowd, D. Blake, and G. D. Coughlan. Longevity hedge effectiveness: A decomposition. *Quantitative Finance*, 14(2):217–235, 2014.

A. J. Cairns, D. Blake, K. Dowd, G. D. Coughlan, D. Epstein, A. Ong, and I. Balevich. A quantitative comparison of stochastic mortality models using data from england and wales and the united states. *North American Actuarial Journal*, 13(1):1–35, 2009.

Y. Chang and M. Sherris. Longevity risk management and the development of a value-based longevity index. *Risks*, 6(1):10, 2018.

J. H. Christensen, J. A. Lopez, and G. D. Rudebusch. Inflation expectations and risk premiums in an arbitrage-free model of nominal and real bond yields. *Journal of Money, Credit and Banking*, 42(s1):143–178, 2010.

J. H. Christensen, F. X. Diebold, and G. D. Rudebusch. The affine arbitrage-free class of nelson–siegel term structure models. *Journal of Econometrics*, 164(1):4–20, 2011.

G. Coughlan. Longevity risk transfer: Indices and capital market solutions. *The Handbook of Insurance-Linked Securities*, pages 261–281, 2009.

G. Coughlan, D. Epstein, A. Sinha, and P. Honig. q-forwards: Derivatives for transferring longevity and mortality risks. *JPMorgan Pension Advisory Group, London, July*, 2, 2007.

G. D. Coughlan, M. Khalaf-Allah, Y. Ye, S. Kumar, A. J. Cairns, D. Blake, and K. Dowd. Longevity hedging 101: A framework for longevity basis risk analysis and hedge effectiveness. *North American Actuarial Journal*, 15(2):150–176, 2011.

C. De Rosa, E. Luciano, and L. Regis. Basis risk in static versus dynamic longevity-risk hedging. *Scandinavian Actuarial Journal*, 2017(4):343–365, 2017.

Deutsche Börse. `https://deutsche-boerse.com/dbg-de/`, 2018.

F. X. Diebold and C. Li. Forecasting the term structure of government bond yields. *Journal of econometrics*, 130(2):337–364, 2006.

A. V. Egorov, H. Li, and D. Ng. A tale of two yield curves: Modeling the joint term structure of dollar and euro interest rates. *Journal of Econometrics*, 162(1):55–70, 2011.

I. V. Girsanov. On transforming a certain class of stochastic processes by absolutely continuous substitution of measures. *Theory of Probability & Its Applications*, 5(3): 285–301, 1960.

S. Haberman, P. Millossovich, V. Kaishev, A. Villegas, S. Baxter, A. Gaches, S. Gunnlaugsson, and M. Sison. Longevity basis risk a methodology for assessing basis risk. `https://www.actuaries.org.uk/documents/longevity-basis-risk-methodology-assessing-basis-risk`, 2014.

Human Mortality Database. University of California, Berkeley (USA), and Max Planck Institute for Demographic Research (Germany). `www.mortality.org/`, 2018.

International Monetary Fund. Global financial stability report. *World Economic and Financial Surveys*, 2012.

P. Jevtić and L. Regis. A continuous-time stochastic model for the mortality surface of multiple populations. *Insurance: Mathematics and Economics*, 88:181–195, 2019. URL `https://doi.org/10.1016/j.insmatheco.2019.07.001`.

P. Jevtić, E. Luciano, and E. Vigna. Mortality surface by means of continuous time cohort models. *Insurance: Mathematics and Economics*, 53(1):122–133, 2013.

Joint Forum. Longevity risk transfer markets: market structure, growth drivers and impediments, and potential risks. `https://www.bis.org/publ/joint31.pdf`, 2013.

R. E. Kalman. A new approach to linear filtering and prediction problems. *Journal of Basic Engineering*, 82(1):35–45, 1960.

J. Li, J. S.-H. Li, L. Tickle, and C. I. Tan. Assessing Basis Risk for Longevity Transactions. https://www.actuaries.org.uk/documents/longevity-basis-risk-phase-2-report, 2017.

J. Li, J. S.-H. Li, C. I. Tan, and L. Tickle. Assessing basis risk in index-based longevity swap transactions. *Annals of Actuarial Science*, 13(1):166–197, 2019.

J. S.-H. Li and M. R. Hardy. Measuring basis risk in longevity hedges. *North American Actuarial Journal*, 15(2):177–200, 2011.

Life and Longevity Markets Association. https://llma.org/index/index-description/, 2018.

J. Loeys, N. Panigirtzoglou, and R. M. Ribeiro. Longevity: A market in the making. https://www.jpmorgan.com/cm/BlobServer/lifemetrics_technical.pdf?blobcol=urldata&blobtable=MungoBlobs&blobkey=id&blobwhere=1158472448701&blobheader=application%2Fpd, 2007.

E. Luciano, L. Regis, and E. Vigna. Single-and cross-generation natural hedging of longevity and financial risk. *Journal of Risk and Insurance*, 84(3):961–986, 2017.

J. Mosher and P. Sagoo. Longevity: Parallels with the past. http://www.theactuary.com/archive/old-articles/part-4/longevity-3A-parallels-with-the-past/, 2011.

C. R. Nelson and A. F. Siegel. Parsimonious modeling of yield curves. *Journal of business*, pages 473–489, 1987.

E. Panopoulou and T. Pantelidis. The fisher effect in the presence of time-varying coefficients. *Computational Statistics & Data Analysis*, 100:495–511, 2016.

A. Renshaw and S. Haberman. Lee–carter mortality forecasting: A parallel generalized linear modelling approach for england and wales mortality projections. *Journal of the Royal Statistical Society: Series C (Applied Statistics)*, 52(1):119–137, 2003.

M. Sherris. Australian longevity index: A technical note. https://www.business.unsw.edu.au/research-site/australianinstituteforpopulationageingresearch-site/Documents/M.%20Sherris%20-%20Australian%20Longevity%20Index%20-%20A%20Technical%20Note.pdf, 2009.

Small Area Income and Poverty Estimates Program. United States Census Bureau. https://www.census.gov/en.html, 2018.

P. Sweeting. Longevity indices and pension fund risk. https://kar.kent.ac.uk/47883/, 2010.

Towers Watson. Longevity hedging the next stop on your ldi journey. https://www.towerswatson.com/DownloadMedia.aspx?media=%7B5D249CF2-99D5-42CF-8D8D-B3EF349427F9%7D, 2013.

United States Mortality Database. University of California, Berkeley (USA). https://usa.mortality.org/, 2018.

M. Uribe. The neo-fisher effect: Econometric evidence from empirical and optimizing models. Technical report, National Bureau of Economic Research, 2018.

A. M. Villegas, S. Haberman, V. K. Kaishev, and P. Millossovich. A comparative study of two-population models for the assessment of basis risk in longevity hedges. *ASTIN Bulletin: The Journal of the IAA*, 47(3):631–679, 2017.

Willis Towers Watson. Global pension assets study 2018. `https://www.willistowerswatson.com/-/media/WTW/Images/Press/2018/01/Global-Pension-Asset-Study-2018-Japan.pdf`, 2018.

S. Wills and M. Sherris. Securitization, structuring and pricing of longevity risk. *Insurance: Mathematics and Economics*, 46(1):173–185, 2010.

Y. Xu, M. Sherris, and J. Ziveyi. Market price of longevity risk for a multi-cohort mortality model with application to longevity bond option pricing. *Journal of Risk and Insurance*, 2019.

Appendix

A Kalman Filter for the Joint Affine Term Structure Model for Mortality

Xu et al. (2019) show that the measurement equation is

$$\vec{\mu}_{x,t} = B\vec{X}_t - \vec{A} + \vec{\epsilon}_t, \qquad \vec{\epsilon}_t \sim N_{2k}(\vec{0}, H),$$

where

$$\vec{\mu}_{x,t} = \begin{bmatrix} \bar{\mu}^R_{x,t}(\tau_1) \\ \vdots \\ \bar{\mu}^R_{x,t}(\tau_k) \\ \bar{\mu}^B_{x,t}(\tau_1) \\ \vdots \\ \bar{\mu}^B_{x,t}(\tau_k) \end{bmatrix}, \qquad B = \begin{bmatrix} \frac{1-e^{-\phi_1\tau_1}}{\phi_1\tau_1} & \frac{1-e^{-\phi_2\tau_1}}{\phi_2\tau_1} & 0 \\ \vdots & \vdots & \vdots \\ \frac{1-e^{-\phi_1\tau_k}}{\phi_1\tau_k} & \frac{1-e^{-\phi_2\tau_k}}{\phi_2\tau_k} & 0 \\ \frac{1-e^{-\phi_1\tau_1}}{\phi_1\tau_1} & 0 & \frac{1-e^{-\phi_3\tau_1}}{\phi_3\tau_1} \\ \vdots & \vdots & \vdots \\ \frac{1-e^{-\phi_1\tau_k}}{\phi_1\tau_k} & 0 & \frac{1-e^{-\phi_3\tau_k}}{\phi_3\tau_k} \end{bmatrix}, \qquad X_t = \begin{bmatrix} C_t \\ R_t \\ B_t \end{bmatrix},$$

$$A = \begin{bmatrix} \frac{1}{2\tau_1}\sum_{i=1,2}\frac{\sigma_i^2}{\phi_i^3}[\frac{1}{2}(1-e^{-2\phi_i\tau_1}) - 2(1-e^{-\phi_i\tau_1}) + \phi_i\tau_1] \\ \vdots \\ \frac{1}{2\tau_k}\sum_{i=1,2}\frac{\sigma_i^2}{\phi_i^3}[\frac{1}{2}(1-e^{-2\phi_i\tau_k}) - 2(1-e^{-\phi_i\tau_k}) + \phi_i\tau_k] \\ \frac{1}{2\tau_1}\sum_{i=1,3}\frac{\sigma_i^2}{\phi_i^3}[\frac{1}{2}(1-e^{-2\phi_i\tau_1}) - 2(1-e^{-\phi_i\tau_1}) + \phi_i\tau_1] \\ \vdots \\ \frac{1}{2\tau_k}\sum_{i=1,3}\frac{\sigma_i^2}{\phi_i^3}[\frac{1}{2}(1-e^{-2\phi_i\tau_k}) - 2(1-e^{-\phi_i\tau_k}) + \phi_i\tau_k] \end{bmatrix}.$$

Here, H is the (diagonal) covariance matrix of the normal error terms and k is the number of ages in the mortality dataset.

The state transition equation is given by

$$\vec{X}_t = \Psi\vec{X}_{t-1} + \vec{\eta}_t, \qquad \vec{\eta}_t \sim N_3(\vec{0}, Q),$$

where

$$\Psi = \begin{bmatrix} e^{-\psi_1} & 0 & 0 \\ 0 & e^{-\psi_2} & 0 \\ 0 & 0 & e^{-\psi_3} \end{bmatrix}, \qquad Q = \begin{bmatrix} \frac{\sigma_1^2}{2\psi_1}(1-e^{-2\psi_1}) & 0 & 0 \\ 0 & \frac{\sigma_2^2}{2\psi_2}(1-e^{-2\psi_2}) & 0 \\ 0 & 0 & \frac{\sigma_3^2}{2\psi_3}(1-e^{-2\psi_3}) \end{bmatrix}.$$

B M7-M5 Model

The M7-M5 model is adopted as the discrete-time two population mortality model.

The M7 model (Cairns et al., 2009) is used for reference population component, that is

$$\text{logit}(q_{x,t}^R) = \kappa_{t,1}^R + (x-\bar{x})\kappa_{t,2}^R + ((x-\bar{x})^2 - \sigma_x^2)\kappa_{t,3}^R + \gamma_{t-x}^R,$$

where $q_{x,t}^R$ is the year t age x mortality rate in the reference population, $\kappa_{t,1}^R$, $\kappa_{t,2}^R$ and $\kappa_{t,3}^R$ are latent-time varying factors corresponding to the mortality curve's level, slope and curvature respectively and γ_{t-x}^R is the cohort effect for those born in year $t-x$. $\bar{x}$ and σ_x^2 denote the sample age mean and sample age variance respectively.

The difference between the book and reference population mortality rates is modelled as

$$\text{logit}(q_{x,t}^B) - \text{logit}(q_{x,t}^R) = \kappa_{t,1}^B + (x-\bar{x})\kappa_{t,2}^B,$$

where $q_{x,t}^B$ is year t age x mortality rate in the book population, $\kappa_{t,1}^B$ and $\kappa_{t,2}^B$ are latent-time varying factors explaining the difference in logit mortality rates and $\bar{x}$ is the sample age mean.

To generate future mortality rate forecasts and simulations in the reference population, the factors $\kappa_{t,1}^R$, $\kappa_{t,2}^R$ and $\kappa_{t,3}^R$ are modelled as a multivariate random walk with drift

$$\begin{bmatrix} \kappa_{t,1}^R \\ \kappa_{t,2}^R \\ \kappa_{t,3}^R \end{bmatrix} = \begin{bmatrix} \mu_1^R \\ \mu_2^R \\ \mu_3^R \end{bmatrix} + \begin{bmatrix} \kappa_{t-1,1}^R \\ \kappa_{t-1,2}^R \\ \kappa_{t-1,3}^R \end{bmatrix} + \begin{bmatrix} \epsilon_{t,1}^R \\ \epsilon_{t,2}^R \\ \epsilon_{t,3}^R \end{bmatrix}, \qquad \begin{bmatrix} \epsilon_{t,1}^R \\ \epsilon_{t,2}^R \\ \epsilon_{t,3}^R \end{bmatrix} \sim N_3(\vec{0}, \Sigma),$$

where μ_1^R, μ_2^R, and μ_3^R are the constant drift parameters and $\epsilon_{t,1}^R$, $\epsilon_{t,2}^R$ and $\epsilon_{t,3}^R$ are error terms that follow a multivariate normal distribution with a mean vector $\vec{0}$ and a covariance matrix Σ.

To generate future mortality rate projections for the book population, the factors $\kappa_{t,1}^B$ and $\kappa_{t,2}^B$ are modelled as a first order vector auto-regression process, VAR(1)

$$\begin{bmatrix} \kappa_{t,1}^B \\ \kappa_{t,2}^B \end{bmatrix} = \begin{bmatrix} \phi_1^B \\ \phi_2^B \end{bmatrix} + \begin{bmatrix} \phi_{1,1}^B & \phi_{1,2}^B \\ \phi_{2,1}^B & \phi_{2,2}^B \end{bmatrix} \begin{bmatrix} \kappa_{t-1,1}^B \\ \kappa_{t-1,2}^B \end{bmatrix} + \begin{bmatrix} \epsilon_{t,1}^B \\ \epsilon_{t,2}^B \end{bmatrix}, \qquad \begin{bmatrix} \epsilon_{t,1}^B \\ \epsilon_{t,2}^B \end{bmatrix} \sim N_2(\vec{0}, \Phi),$$

where ϕ_1^B, ϕ_2^B, $\phi_{1,1}^B$, $\phi_{1,2}^B$, $\phi_{2,1}^B$ and $\phi_{2,2}^B$ are constant parameters and $\epsilon_{t,1}^B$ and $\epsilon_{t,2}^B$ are error terms that follow a multivariate normal distribution with a mean vector $\vec{0}$ and a covariance matrix Φ. We also assume independence between these error terms and those of the reference population time series model.

C Kalman Filter for the Dynamic Nelson-Siegel Model

The measurement equation is

$$\vec{y}_t^N = B^N \vec{X}_t^N + \vec{\epsilon}_t^N, \qquad \vec{\epsilon}_t^N \sim N_n(\vec{0}, H^N),$$

where

$$\vec{y}_t^N = \begin{bmatrix} y_t^N(\tau_1) \\ \vdots \\ y_t^N(\tau_n) \end{bmatrix}, \qquad B^N = \begin{bmatrix} 1 & \frac{1-e^{-\lambda^N \tau_1}}{\lambda^N \tau_1} & \frac{1-e^{-\lambda^N \tau_1}}{\lambda^N \tau_1} - e^{-\lambda^N \tau_1} \\ \vdots & \vdots & \vdots \\ 1 & \frac{1-e^{-\lambda^N \tau_n}}{\lambda^N \tau_n} & \frac{1-e^{-\lambda^N \tau_n}}{\lambda^N \tau_n} - e^{-\lambda^N \tau_n} \end{bmatrix}, \qquad \vec{X}_t^N = \begin{bmatrix} L_t^N \\ S_t^N \\ C_t^N \end{bmatrix},$$

$$\vec{\epsilon}_t^N = \begin{bmatrix} \epsilon_t^N(\tau_1) \\ \vdots \\ \epsilon_t^N(\tau_n) \end{bmatrix},$$

H^N is the (diagonal) covariance matrix of the normal error terms and $n = 11$ observed maturities.

The state transition equation is given by

$$[\vec{X}_t^N - \vec{\theta}^N] = \kappa^N [\vec{X}_{t-1}^N - \vec{\theta}^N] - \vec{\eta}_t, \qquad \vec{\eta}_t \sim N_3(\vec{0}, Q^N),$$

where

$$\vec{\theta}^N = \begin{bmatrix} \theta_L^N \\ \theta_S^N \\ \theta_C^N \end{bmatrix}, \qquad \kappa^N = \begin{bmatrix} e^{-\kappa_1^N \Delta t} & 0 & 0 \\ 0 & e^{-\kappa_2^N \Delta t} & 0 \\ 0 & 0 & e^{-\kappa_3^N \Delta t} \end{bmatrix},$$

$$Q^N = \begin{bmatrix} \frac{\sigma_1^2(1-e^{-2\kappa_1^N \Delta t})}{2\kappa_1^N} & 0 & 0 \\ 0 & \frac{\sigma_2^2(1-e^{-2\kappa_2^N \Delta t})}{2\kappa_2^N} & 0 \\ 0 & 0 & \frac{\sigma_3^2(1-e^{-2\kappa_3^N \Delta t})}{2\kappa_3^N} \end{bmatrix}$$

and $\Delta t = \frac{1}{12}$ (for monthly data).

D Numerical Optimisation

Following the approach in Li et al. (2017), the swap weight parameter w_0 is chosen in order to minimise the variance of the quantity

$$\sum_{i=1}^{\omega-x} l_{x+i,t+i}^B \times P_R(t, t+i) + w_0 \sum_{i=1}^{\omega-x-1} (I_{x+i,t+i} - I_{x+i,t+i}^f) \times P_N(t, t+i),$$

with respect to simulated future mortality, interest rate and inflation experience.